IL NUOVO CIMENTO Vol. 33 C, N. 1 Gennaio-Febbraio 2010
DOI 10.1393/ncc/i2010-10573-5

Colloquia: ICTT2009

Numerical simulation of coupled electron devices and circuits by the MEP hydrodynamical model for semiconductors with crystal heating

V. Romano([1]) and A. Rusakov([2])

([1]) *Dipartimento di Matematica e Informatica, Università di Catania - Viale A. Doria 6 I-95125 Catania, Italy*
([2]) *Bergische University of Wuppertal - Gaussstr. 20, Wuppertal, Germany*

(ricevuto il 31 Ottobre 2009; approvato il 13 Gennaio 2010; pubblicato online l'8 Marzo 2010)

Summary. — Solutions of a new 2d semiconductor numerical model describing the electron transport in semiconductors coupled with the heating of the crystal lattice are presented. The model equations have been obtained with the use of the maximum entropy principle. Numerical simulations of a nanoscale MOSFET and inverter circuit are presented and the influence of self-heating on the electrical characteristics is analyzed.

PACS 63.20.-e – Phonons in crystal lattices.
PACS 46.15.-x – Computational methods in continuum mechanics.
PACS 85.35.-p – Nanoelectronic devices.
PACS 47.11.St – Multi-scale methods.

1. – Introduction

Influence of the thermal heating of the carriers and crystal lattice on the performance of semiconductor devices increases as the miniaturization is more and more progressing and density of the transistor increases. Consequently the analysis of the thermal effects becomes more and more important for the validation of device and circuit behavior. Therefore new approaches are required for analysis of influence of circuit self-heating. Typically in commercial circuit simulators semiconductor devices are modeled with empirical functions but such an approximation might produce not accurate results for nanoscale devices. In this paper a numerical integration of a new coupled electro-thermal model for semiconductors, developed recently in [1, 2], is performed. At macroscopic level, several heuristic models of lattice heating have been proposed in the literature. They are represented by the lattice energy balance equation and differ for the proposed form of thermal conductivity and energy production, *e.g.* [3-8]. Here we consider a macroscopic model which has been formulated starting from the semiclassical

description based on the Boltzmann equations describing the electron-phonon system. The closure relations have been obtained with the maximum entropy principle (hereafter MEP). The electrons are described with the 8-moment system. The phonons are considered as two populations: acoustic and non polar optical. The non-polar optical phonons are described with the Bose-Einstein distribution while the acoustic ones are described by the MEP distribution function in the 9-moment approximation. Explicit constitutive relations have been obtained with coefficients depending on the electron energy W and crystal temperature T_L and related to the scattering parameters (see [1] for more details).

In this paper a new 2D coupled electro-thermal numerical model is developed and simulations are performed. Results for a nanoscale MOSFET coupled electro-thermally with a circuit are presented and the influence of the thermal effects on the electrical performance is analyzed.

2. – Mathematical model

The model is represented by the set of equations

$$\frac{\partial n}{\partial t} + \operatorname{div}(n\,\mathbf{V}) = -R, \tag{1}$$

$$\frac{\partial p}{\partial t} + \operatorname{div}(p\,\mathbf{V}_p) = -R, \tag{2}$$

$$\frac{\partial (nW)}{\partial t} + \operatorname{div}(n\,\mathbf{S}) + nq\mathbf{V}\cdot\nabla\phi = nC_W, \tag{3}$$

$$\rho c_V \frac{\partial T_L}{\partial t} - \operatorname{div}[K(T_L)\nabla T_L] = H, \tag{4}$$

$$\mathbf{E} = -\nabla\phi, \quad \epsilon\Delta\phi = -q(N_D - N_A - n + p). \tag{5}$$

n and p are the electron and hole density, respectively, W is the electron energy, T_L the lattice temperature, ϕ the electrostatic potential and $\mathbf{E} = -\nabla\phi$ the electric field. N_D and N_A are the donor and acceptor density, respectively (assumed as known functions of the position). q is the elementary charge, ρ the silicon density, c_V the specific heat, C_W the energy production term, which is in a relaxation form $C_W = -\frac{W-W_0}{\tau_W}$, with $W = 3/2k_BT_L$ and $\tau_W(W)$ the energy relaxation time. k_B is the Boltzmann constant and ϵ is the dielectric constant.

The closure relations for the electron velocity $\mathbf{V}$, the energy flux $\mathbf{S}$, the thermal conductivity $K(T_L)$ and the crystal energy production term H have been obtained in [1,9] by employing MEP. The holes are described by a standard drift-diffusion model with constant mobility. $\mathbf{V}_p$ is the hole velocity.

In the MEP model the expressions of the electron velocity $\mathbf{V}$ and the energy flux $\mathbf{S}$ are given by

$$\mathbf{V} = D_{11}(W,T_L)\,\nabla\log n + D_{12}(W,T_L)\,\nabla W + D_{13}(W,T_L)\,\nabla\phi, \tag{6}$$

$$\mathbf{S} = D_{21}(W,T_L)\,\nabla\log n + D_{22}(W,T_L)\nabla\, W + D_{23}(W,T_L)\,\nabla\phi, \tag{7}$$

with

$$D_{11}(W,T_L) = D_V\left[c_{12}^{(e)}F - c_{22}^{(e)}U\right], \qquad D_{12}(W,T_L) = D_V\left[c_{12}^{(e)}F' - c_{22}^{(e)}U'\right], \tag{8}$$

$$D_{13}(W,T_L) = D_V\left[c_{22}^{(e)}e - c_{12}^{(e)}eG\right], \qquad D_V(W,T_L) = \frac{1}{c_{12}^{(e)}c_{21}^{(e)} - c_{22}^{(e)}c_{11}^{(e)}}, \tag{9}$$

$$D_{21}(W,T_L) = D_S\left[c_{11}^{(e)}F - c_{21}^{(e)}U\right], \qquad D_{22}(W,T_L) = D_S\left[c_{11}^{(e)}F' - c_{21}^{(e)}U'\right], \tag{10}$$

$$D_{23}(W,T_L) = D_S\left[c_{21}^{(e)}e - c_{11}^{(e)}eG\right], \qquad D_S(W,T_L) = \frac{1}{c_{22}^{(e)}c_{11}^{(e)} - c_{12}^{(e)}c_{21}^{(e)}}. \tag{11}$$

The coefficients $c_{ij}^{(e)}$ arise from the momentum and energy-flux production terms and depend on W and T_L. The complete expressions are reported in [1]. Since the electron production terms are slowly changing with respect to $k_B T_L$, we adopt the simplification that they are evaluated at $T_L = 300\,\mathrm{K}$.

The phonon energy production is given by

$$H = -(1+P_S)\,n\,C_W + P_S\;\mathbf{J}\cdot\mathbf{E}, \tag{12}$$

where $P_S = -c^2\,\tau_R\,c_{12}^{(p)}$ plays the role of a thermopower coefficient and τ_R is the phonon relaxation time in resistive processes. In [1, 9] a more general model for H has been proposed but in the steady state the two expressions are equivalent.

R is the generation-recombination term (see [10] for a complete review) which splits into the Shockley-Read-Hall (SRH) and the Auger contribution (AU): $R = R^{\mathrm{SRH}} + R^{\mathrm{AU}}$ with

$$R^{\mathrm{SRH}} = (np - n_i n_i)/(\tau_p(n+n_1) + \tau_n(p+p_1)), \qquad R^{\mathrm{AU}} = (C_{cn}n + C_{cp}p)(np - n_i n_i).$$

We will take the values $C_{cn} = 2.8\times10^{-31}\,\mathrm{cm}^6\,\mathrm{s}^{-1}$ and $C_{cp} = 9.9\times10^{-32}\,\mathrm{cm}^6\,\mathrm{s}^{-1}$. In our numerical experiments we set $n_1 = p_1 = n_i$, n_i being the intrinsic concentration. The expressions of τ_p and τ_n we will use are [10]

$$\tau_n = \frac{\tau_{n0}}{1 + \frac{N_D(x)+N_A(x)}{N_n^{ref}}}, \qquad \tau_p = \frac{\tau_{p0}}{1 + \frac{N_D(x)+N_A(x)}{N_p^{ref}}}, \tag{13}$$

where $\tau_{n0} = 3.95\times10^{-4}\,\mathrm{s}$, $\tau_{p0} = 3.25\times10^{-5}\,\mathrm{s}$, $N_n^{\mathrm{ref}} = N_p^{\mathrm{ref}} = 7.1\times10^{15}\,\mathrm{cm}^{-3}$.

On source and drain contacts the Robin boundary condition $-k_L\frac{\partial T_L}{\partial n} = R_{\mathrm{th}}^{-1}(T_L - T_{\mathrm{env}})$ is assumed, R_{th} being the thermal resistivity of the contact and T_{env} the environment temperature. We use no-flux condition for temperature on the lateral boundary and oxide silicon interface and Dirichlet condition on the bulk contact. The electron energy on the source, drain and bulk contact is set equal to lattice energy. Other boundary conditions in the MOSFET model are described in [11].

3. – The numerical method

Crystal lattice temperature T_L changes much slower than other variables. For instance the typical relaxation time for the temperature in our simulations is several thousand picoseconds, while relaxation time of the other fields is several picoseconds. We exploit

this double-scale behavior applying a variant of the multirate integration scheme [12] which is a popular choice in coupled electro-thermal circuit simulation [13]. For the analysis of the transient response of the model we solve the balance equations by adopting the following multirate integration scheme:

– Step 1. We integrate the balance equations for electrons and holes, with the crystal lattice energy and the electric field, obtained by solving the Poisson equation, frozen at the previous time step, obtaining the electron and hole density and energy at the next time step. Schematically this step can be written as

$$\frac{\partial \mathcal{U}^k}{\partial t} + F\left(\mathcal{U}^k, \phi^{k-1}, T_L^{k-1}\right) = 0, \tag{14}$$

with $\mathcal{U} = (n, p, W, \phi)$, where $k = 1, \ldots, N$ is the index of the integration interval $[t_{k-1}, t_k]$, $t_k = t_{k-1} + \Delta t$, Δt being the time size of the synchronization window.

– Step 2. We integrate the lattice energy balance equation with n and W given by the step 1:

$$\rho c_V \frac{\partial T_L^k}{\partial t} - \operatorname{div}[K(T_L^k)\nabla T_L] = H(\mathcal{U}^k, T_L^k). \tag{15}$$

For step 1 and step 2 different time steps for numerical integration over the interval $[t_{k-1}, t_k]$ are used. Typically the time step for integration of (15) we can use is 100 times larger than the time step for (14). This sequence can be considered as steps of a splitting technique [14] with time step Δt and we can expect that such a numerical scheme is stable and provides us with a first-order approximation with respect to time.

The numerical scheme for solution of electrical part is based on an exponential fitting like that employed in the Scharfetter-Gummel scheme for the drift-diffusion model of semiconductors. The basic idea is to split the particle and energy density currents as the difference of two terms. Each of them is written by introducing suitable mean mobilities in order to get expressions of the currents similar to those arising in other energy-transport models known in the literature. A simple explicit discretization in time with constant time step proves satisfactorily efficient avoiding the problem related to the high nonlinear coupling of the discretized equations. The model equations are spatially discretized on a regular grid. The details of numerical scheme can be found in [11].

To solve a lattice energy equation (15) a coordinate splitting technique [14] is used. For the space approximation in every direction an implicit time scheme with the three points stencil is chosen. The obtained linear system can be solved efficiently with tridiagonal matrix factorization procedure. We remark that usage of the implicit time scheme for lattice energy operator significantly improves overall simulation time.

4. – Numerical simulation of crystal heating in MOSFET

In this section we present the numerical simulations of the heating of the crystal lattice in a MOSFET described by the MEP model and a solution of an inverter circuit containing a nano-scale MOSFET. For the single MOSFET the steady-state solution is analyzed while for the coupled device-circuit system the transient is simulated.

Concerning the physical parameters, we have modeled the thermal conductivity with the fitting formula $K(T_L) = 1.5486(T_L/300\,\mathrm{K})^{-4/3}\,\mathrm{V\,A/cm\,K}$, assumed $c_V = 703\,\mathrm{m^2/s^2\,K}$ (see [10]) and set $T_{\mathrm{env}} = 300\,\mathrm{K}$. The hole low field mobility is set equal to $500\,\mathrm{cm^2/V\,s}$.

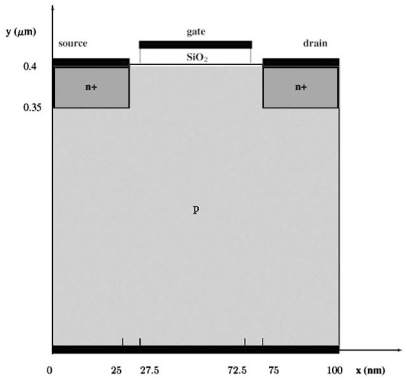

Fig. 1. – Schematic representation of a bidimensional MOSFET.

The shape of the device is depicted in fig. 1. The length of the channel is 50 nm, the gate length is 45 nm, source and drain are 25 nm long. The source and drain depths are $0.1\,\mu$m. The gate oxide is 5 nm thick. The substrate thickness is $0.4\,\mu$m. The environment temperature T_{env} is set equal to 300 K. In our numerical experiments we take the thermal resistivity $R_{\text{th}} = 10^{-8}\,\text{Km}^2/\text{W}$ as in [15]. The doping concentration is

$$N_D(x) - N_A(x) = \begin{cases} 10^{17}\,\text{cm}^{-3} \text{ in the } n^+ \text{ regions} \\ -10^{14}\,\text{cm}^{-3} \text{ in the } p \text{ region} \end{cases} \tag{16}$$

with abrupt junctions. The gate voltage is $V_{DG} = 0.8\,\text{V}$.

The steady-state solutions of the electron density and energy and the electrostatic potential, have a qualitative behaviour similar to the case when T_L is kept constant at the equilibrium value (the interested reader can see [11]), as shown in figs. 2-4.

The stationary solution of the crystal temperature is plotted in fig. 5. In the most part of the device there is a clear departure of the crystal temperature from the equilibrium

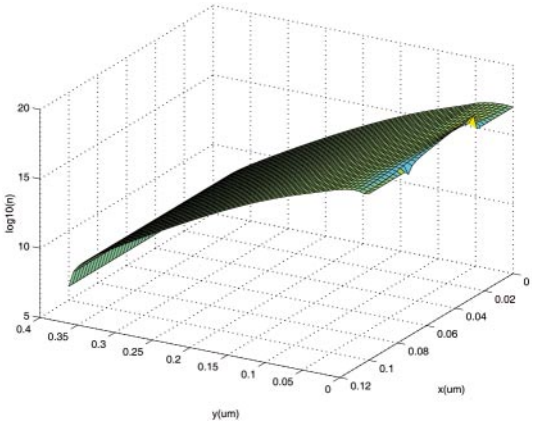

Fig. 2. – Stationary solution for electron density in MOSFET with 50 nm channel in logarithm scale.

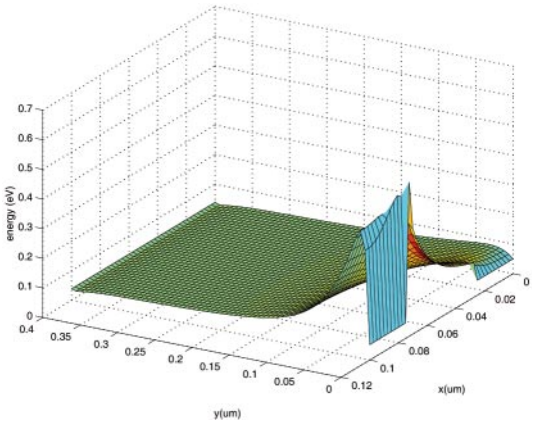

Fig. 3. – Stationary solution for electron energy in MOSFET with 50 nm channel.

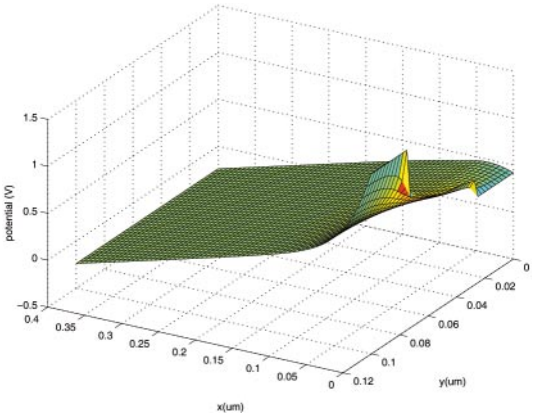

Fig. 4. – Stationary solution for voltage in MOSFET with 50 nm channel.

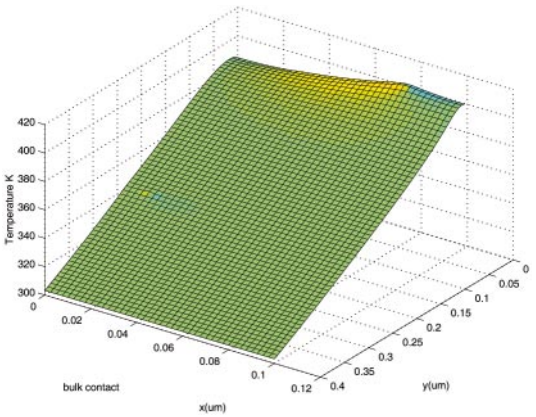

Fig. 5. – Stationary solution for lattice temperature distribution in MOSFET with 50 nm channel length.

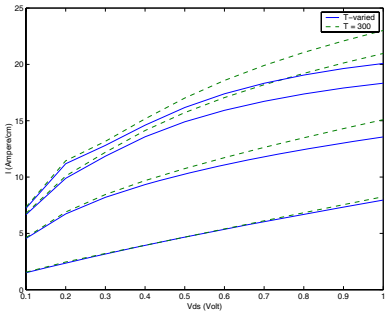

Fig. 6. – Drain current with constant and simulated lattice temperature for MOSFET with 50 nm channel $n_+ = 10^{18}\,\mathrm{cm}^{-3}$, $R_{\mathrm{th}} = 10^{-8}$. $V_{DG} = 0.4, 0.6, 0.8, 0.9\,\mathrm{V}$. The current increases as V_{DG} increases.

value. In particular the lattice temperature raises more than 400 K in the area near the gate where there is the maximum for the electron energy. This is of crucial importance in the design of electron devices because the presence of hot spot can damage the MOSFET. Such an effect is not relevant in devices of order of microns or few tenths of micron, but by shrinking the dimension of the device to nanoscales, the crystal heating effects have also a non-negligible influence on the current through the device. In fig. 6 current voltage characteristics for the device with $n_+ = 10^{17}\,\mathrm{cm}^{-3}$ are shown. As the electric field increases there is a significant difference between the characteristic curves with constant lattice temperature and those with varying T_L, influencing the performance of the transistor, especially when coupled with other devices in a complex circuit.

To analyze this fact we simulate the heating of a transistor in the electrical circuit representing an inverter. The inverter circuit is plot in fig. 7. Input voltage on the gate contact is (in Volt) $V_{\mathrm{in}} = 0.3\cos(\omega t) + 0.5$, with frequency $\omega = 2\pi\ 10^9\,\mathrm{rad/s}$ and power voltage $V_{dd} = 1\,\mathrm{V}$. Load capacitance $C = 0.1\,\mathrm{fF}$ and $R = 2\ 10^3\,\Omega$. The width of the transistor (length in the orthogonal direction with respect to the considered 2D cross-section) is set equal to 200 nm. Modified nodal analysis gives us for the output voltage V_{out}:

$$C\frac{\mathrm{d}V_{\mathrm{out}}}{\mathrm{d}t} + \frac{V_{\mathrm{out}} - V_{dd}}{R} + j(V_{\mathrm{in}}, V_{\mathrm{out}}, t) = 0, \tag{17}$$

where current through the transistor $j(V_{\mathrm{in}}, V_{\mathrm{out}}, t)$ is computed by the energy-transport model. We refer for instance to [15] for details of device-circuits coupled modeling

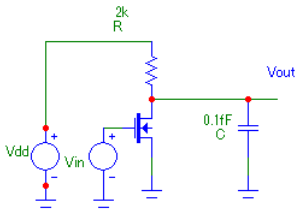

Fig. 7. – Simulated inverter circuit.

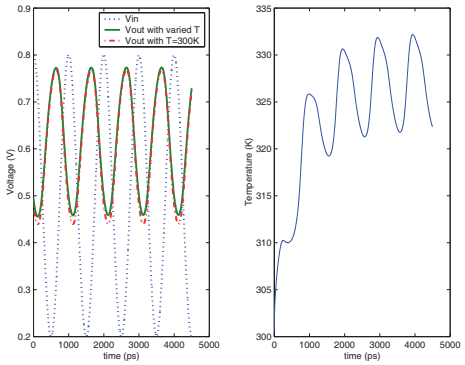

Fig. 8. – On the left input and output voltages *vs.* time. On the right maximum value of the lattice temperature in the MOSFET *vs.* time.

algorithm. The output voltage simulated with and without transistor self-heating and maximum temperature in the transistor are plot in fig. 8. One can see that lattice temperature in the transistor does not achieve 400 K as we have observed in the single transistor simulation. It can be explained with smaller average voltage at the gate and consequently smaller average electrical field. However there is still a shift in the minimum values of the output voltage and a clear indication of the crystal heating.

* * *

The authors acknowledge the financial support by the EU Marie Curie RTN project COMSON grant n. MRTN-CT-2005-019417.

REFERENCES

[1] Romano V. and Zwierz M., *Electron-phonon hydrodynamical model for semiconductors*, preprint (2008).
[2] Romano V., *Math. Methods Appl. Sci.*, **24** (2001) 439.
[3] Gaur S. P. and Navon D. H., *IEEE Trans. Electron Devices*, ED-23 (1976) 50.
[4] Sharma D. K. and Ramanthan K. V., *IEEE Electron Devices Lett.*, EDL-4 (1983) 362.
[5] Adler M. S., *IEEE Trans. Electron Devices*, ED-25 (1979) 16.
[6] Chryssafis A. and Love W., *Solid-State Electron.*, **22** (1978) 249.
[7] Wachutka G., *IEEE Trans. Comput.-Aided Des.*, **9** (1990) 1141.
[8] Dreyer W. and Struchtrup H., *Contin. Mech. Thermodyn.*, **5** (1993) 3.
[9] Romano V. and Scordia C., *Simulations of an electron-phonon hydrodynamical model based on the maximum entropy principle*, in *Proceedings SCEE 2008*, in press.
[10] Selberherr S., *Analysis and Simulation of Semiconductor Devices* (Springer-Verlag, Wien-New York) 1984.
[11] Romano V., *J. Comput. Phys.*, **221** (2007) 439.
[12] Guenther M. and Rentrop P., *Appl. Num. Math.*, **13** (1993) 83.
[13] Bartel A. and Guenther M., *Multirate co-simulation of first order thermal models in electric circuit design*, *Scientific Computing in Electrical Engineering, Proceedings SCEE 2002*, edited by Schilders W. *et al.* (Springer, Berlin) 2002, pp. 23–28.
[14] Marchuk G. I., *Splitting and Alternating Direction Method*, in *Handbook of Numerical Analysis*, Vol. **1** (1990), pp. 197-462.
[15] Brunk M. and Jüngel A., *SIAM J. Sci. Comput*, **30** (2008) 873.